Research article

Journal of RAMAN SPECTROSCOPY

Received: 26 September 2015 Revised: 21 February 2016 Accepted: 29 February 2016 Published online in Wiley Online Library

(wileyonlinelibrary.com) DOI 10.1002/jrs.4925

Characterisation and classification of automotive clear coats with Raman spectroscopy and chemometrics for forensic purposes

Mark Maric,[a,b,d] Wilhelm van Bronswijk,[b] Kari Pitts[c] and Simon W. Lewis[a,b]*

The clear coats from a collection of automotive paint samples of 139 vehicles, covering a range of Australian and international vehicle manufacturers and sold in Western Australia, were characterised using FT-Raman spectroscopy. Principal component analysis (PCA) revealed 19 distinct classes that were associated with the vehicles' manufacturer and model, and in the case of Australian manufacturers, the years of manufacture. Linear discriminant analysis based on the PCA groupings gave excellent discrimination between the groups with 96.9% of the calibration set and 97.6% of the validation set being correctly classified. Although the sample set comprised only vehicles available in Australia, the methodology used is universal and hence applicable in any jurisdiction that is willing and able to generate a statistically significant data set and maintain and update it as new vehicles appear on the market. A FT-Raman spectroscopy-based database would rapidly provide information regarding vehicle origin and manufacture and hence generate investigative leads for questioned paint samples found at incident sites. Copyright © 2016 John Wiley & Sons, Ltd.

Additional supporting information may be found in the online version of this article at the publisher's web site.

Keywords: automotive clear coats; Raman spectroscopy; principal component analysis; linear discriminant analysis; forensic science

Introduction

Automotive paint in the form of chips or smears is frequently encountered at vehicle-related incidents, such as hit-and-runs and automobile crashes. In some instances, automotive paint may be the only viable form of physical evidence available to forensic examiners, thus making its subsequent analysis imperative to the investigation. Whilst there is no current universal methodology for forensic paint examination, guidelines have been developed by the Scientific Working Group on Materials Analysis[1] and by the American Society for Testing and Materials,[2] in order to provide a framework for the analysis of paint evidence. These techniques include, but are not limited to, microscopical examinations, microspectrophotometry, infrared (IR) spectroscopy, Raman spectroscopy, pyrolysis-gas chromatography/mass spectrometry (Py-GC/MS) and elemental analysis techniques.[1,2]

If a known paint sample is available to the examiner, then comparisons between the questioned paint sample obtained from the scene and the known paint sample are undertaken, using a combination of the analytical techniques mentioned in the preceding texts, along with the use of a database of known references such as Paint Data Query (PDQ).[3,4] However, in instances where a known sample is not available for comparison, such as those involving hit-and-run offences, the physical and chemical characteristics of the questioned sample can be compared to the PDQ database, in order to procure investigative leads. In any case, questioned *versus* known comparisons or use of the PDQ database is heavily reliant on a forensic examiner's interpretation of analytical results, raising serious concerns regarding human error and observer bias. Recent inquiries conducted by the Science and Technology Committee[5] in the UK and the National Academy of Sciences[6] in the USA have revealed that there is the potential for bias in the current interpretational protocols for forensic trace evidence. Specifically, the National Academy of Sciences report identified the need to establish strict rigorous protocols for the interpretation of forensic evidence.[6] Multivariate statistics or chemometrics has the potential to account for this issue by enabling meticulous statistical and scientific approaches to the interpretation of forensic evidence. Chemometrics has been previously utilised in forensic science in order to mitigate bias and partiality in the interpretation of analytical data obtained from trace evidence.[7–9] A combination of principal component analysis (PCA) and linear discriminant analysis (LDA) has been applied in the

* *Correspondence to: Simon W. Lewis, Nanochemistry Research Institute GPO Box U1987, Perth, Western Australia 6845, Australia. E-mail: s.lewis@curtin.edu.au*

a *Nanochemistry Research Institute, GPO Box U1987, Perth, Western Australia, 6845, Australia*

b *Department of Chemistry, Curtin University, GPO Box U1987, Perth, Western Australia, 6845, Australia*

c *ChemCentre, PO Box 1250, Bentley, Western Australia, 6983, Australia*

d *National Centre for Forensic Science, University of Central Florida, PO Box 162367, Orlando, FL, 32816, USA*

discrimination and classification of forensic evidence, including fibres,[10–12] glass,[13,14] inks,[15,16] soil,[17,18] hair,[19] accelerants,[20–22] photocopy and printer toners,[23–26] paper,[27] electrical tapes[28,29] and paint.[30–34]

Specifically, chemometrics has also been shown to be a viable technique for the interpretation of automotive paint evidence. A study by Kochanowski and Morgan used Py-GC/MS with PCA and LDA to characterise and discriminate between 100 automotive paint samples, representing five different colours. The authors concluded that LDA was capable of discriminating between paint samples as a function of their colour and the PCA subplots may enable further differentiation between vehicles of a similar colour, but different make and model.[30] Another study by Liszewski *et al.* utilised ultraviolet microspectrophotometry in conjunction with chemometrics to assess the extent of diversity within a number of original automotive clear coats. Cluster analysis and PCA performed on the resultant data revealed three distinct groupings; however, no correlation could be made between the groupings as a function of the make, model or year of the corresponding vehicles, thus limiting the applicability of the statistical model for procuring investigative leads.[31] Lavine and co-workers have demonstrated the utility of pattern recognition techniques in conjunction with the PDQ database to successfully extract information from FTIR spectra in the database to aid in the generation of investigative leads.[35–41] A recent study conducted by the authors used attenuated total reflectance (ATR) IR spectroscopy to characterise clear coats of over 100 vehicles and then used a combination of PCA and LDA to examine the diversity in the sample population. The authors concluded that the ATR model is capable of differentiating between samples based upon the origin, manufacturer and in some instances the model and year of manufacture of the vehicle.[32]

The following research aims to build upon the knowledge acquired from the previous study by using FT-Raman spectroscopy to characterise the population of automotive clear coats, with subsequent chemometric analysis to interpret the resultant data. Raman spectroscopy has enormous potential for the forensic analysis of paints, owing to its ability to characterise both the organic and inorganic components of the paint system at a very high spatial resolution and with minimal sample preparation.[42,43] Whilst Raman spectroscopy has been extensively applied to the examination of artistic paints (e.g. in instances of art forgery),[44–46] there is less published work in the literature using this technique to characterise architectural[47–49] and automotive paints,[50–52] which are commonly encountered in forensic casework. Furthermore, of the handful of studies that employed Raman spectroscopy to examine automotive paint systems, the majority have used the technique solely to characterise the organic and inorganic pigments in the basecoat or the fillers and extenders in the primer surfacer. De Gelder and co-workers employed Raman spectroscopy to characterise all of the layers, including the clear coat, in automotive paint cross sections.[52] The authors discovered that although reproducible spectra could be obtained from clear coats, the basecoat of the paint system provided the best spectra with which to discriminate between paint samples.[52] Due to the paucity of research in the literature and because IR and Raman spectroscopy are complementary techniques, the following study will explore the potential of Raman spectroscopy in conjunction with chemometric analysis for the characterisation and classification of automotive clear coats. This work has targeted the clear coat as it is almost always encountered as transfer evidence involving motor vehicles. Furthermore, it is also the most easily assessed *in situ* (on vehicles) with handheld instrumentation. The resultant statistical model will enable comparisons to be made to the equivalent model previously generated from ATR data,[32] in order to determine which vibrational spectroscopic technique is better suited to this application.

Experimental

Sampling

All automotive paint exemplars were obtained from a sunroof fitting company (Prestige Sunroofs WA, Australia) from roof panels removed during the process of sunroof installation. The make, model, year and vehicle identification number were recorded for each vehicle. The sample population outlined in this study consisted of 139 individual vehicle samples from new cars with minimal exposure covering a range of Australian and international manufacturers. The sample collection consists of a diverse range of vehicles with 17 different manufacturers and 45 different models being represented, as depicted in Table 1, and incorporates the 130 vehicles used in the previous ATR IR study.[32]

Table 1. A summary of the vehicle type/s, model/s and origin of manufacture for every vehicle in the sample population

Manufacturer	No. of samples		Model(s)	Origin of manufacture
BMW	3		325i/135i Coupe	Germany
Dodge	7	5	Nitro	USA
		2	Journey	Mexico
Ford	17	10	Falcon/Territory	Australia
		5	Focus	Germany
		2	Mondeo	Germany
Holden	38	36	Commodore/ Calais/ Adventra /Caprice/Cruze	Australia
		2	Captiva	South Korea
Holden Special Vehicles	9		Grange/GTS/ Clubsport	Australia
Honda	8	3	Accord	Japan
		2	CRV	Poland
		2	City	Thailand
		1	Civic	UK
Hyundai	5		i30/Elantra	South Korea
Jaguar	1		X-Type	UK
Jeep	3		Cherokee	USA
Mazda	12		Mazda 3/Mazda 6	Japan
Mitsubishi	8	4	Pajero	Japan (Nagoya)
		3	Lancer	Japan (Mizushima)
		1	Colt	Japan
Nissan	5	2	Maxima	Thailand
		2	Navara	Spain
		1	X-Trail	Japan
Saab	2		Saab 93	Sweden
SsangYong	2		Kyron	South Korea
Subaru	5		Impreza	Japan
Suzuki	1		Grand Vitara	Japan
Toyota	13	6	Celica/Corolla/ Prado/Kluger	Japan
		4	Camry	Australia
		3	Hilux	Thailand

Journal of RAMAN SPECTROSCOPY

FT-Raman spectroscopy

Raman spectra were acquired with a Bruker RFS 100 FT-Raman spectrometer (Bruker Optik GmbH, Ettlingen, Germany) equipped with a liquid nitrogen-cooled, high-sensitivity germanium diode detector. A near-IR neodymium-doped yttrium aluminium garnet continuous wave laser, operating with an excitation wavelength of 1064 nm and with a maximum power of 800 mW, was used to characterise the clear coats. Analysis of the clear coat layer was achieved by employing a scalpel to obtain thin shavings of the coating, which were then tightly packed into a stainless steel sample cup. Shavings were obtained from the outer surface of the clear coat, such that the shavings were unaffected by chemical component migration and thus truly representative of the composition of the coating. Five spectra were collected from each sample using 180° back-scattering sampling mode at a focal position of 0.0 mm, over a range of 3600–75 cm^{-1} (Stokes shift), with a spectral resolution of 4 cm^{-1}, and 1024 accumulated scans (~30 min).

Chemometrics

Prior to the use of chemometric techniques, the data was pre-processed in order to eliminate systematic noise and any variation arising from the characterisation of the sample. This was performed by collating all the spectra and assembling them into separate data matrices, whereby every column signified a variable and each row represented a sample. They were then linearly baseline corrected and range normalised (so that the strongest peak is always set to an intensity of 1) and truncated to a range of 1800–600 cm^{-1}. Truncation of the dataset eliminates extraneous variables, such as those pertaining to aliphatic C–H stretches, thus retaining only chemically relevant information from the fingerprint region of the spectra.

Principal component analysis

PCA was performed on the individual pre-processed datasets in order to visualise groupings and enable relationships to be discerned. In both instances, mean-centred data was analysed by PCA using the non-linear iterative partial least squares algorithm. Three-dimensional score plots were generated by using the scores from as many as the first five principal components (PCs), so as to visualise the structure within the datasets. The loadings corresponding to these PCs were then employed to identify characteristic spectral features that give rise to the discrimination between samples.

Linear discriminant analysis

LDA with test set validation was then utilised to generate a discriminant model. In test set validation, the entire spectral datasets were segregated into two independent sets of data: a calibration or training set and a validation set. In each case, the training sets (490 spectra; 98 vehicles) were roughly 2.5 times larger than the validation sets (205 spectra; 41 vehicles). As some groupings in the dataset contained more samples than others, the data was separated in a manner such that the training sets contained roughly 2.5 times more samples per grouping than the validation sets. The training sets were used to generate the discriminant models, whilst the validation sets were then utilised to classify unknown test samples and gauge the predictive performance of the models. This information was presented in a table in the form of a confusion matrix. All pre-processing and subsequent statistical analysis of the data was performed using the Unscrambler® X 10.2 software (CAMO Software AS, Oslo, Norway).

Results and discussion

Raman spectra of automotive clear coats were obtained from 139 different vehicles available in Western Australia. As the vehicles were new, shavings were obtained from the outer surface of the clear coat, such that the shavings were unaffected by chemical component migration and thus truly representative of the composition of the coating. In operational situations where weathering is a concern, samples from within the bulk of the clear coat would need to be sampled. PCA performed on the Raman data matrix (695 spectra) revealed that 96.7% of the total variance in the dataset was accounted for by the first five PCs, as seen in Fig. S1 (Supporting Information). Based upon Fig. S1 (Supporting Information), it can be clearly seen that as many as five PCs could be employed to reconstruct and model the data. Whilst the first three PCs may be capable of adequately describing the data, additional PCs were evaluated, as the spectral variation may be quite subtle.

A three-dimensional score plot generated using the first three PCs indicated that there visually appear to be 19 groupings in the Raman dataset (Fig. 1 and Animation S1 (Supporting Information)). Score plots were also created from a number of combinations of the first five PCs, in order to examine the influence of PC4 and PC5. The fourth and fifth PCs were determined to afford no additional discrimination between samples, thereby justifying the use of only three PCs. The score plot depicted in Fig. 1 illustrates the separation of the data into 19 groupings, with the discrimination between sample groupings again being attributable to common

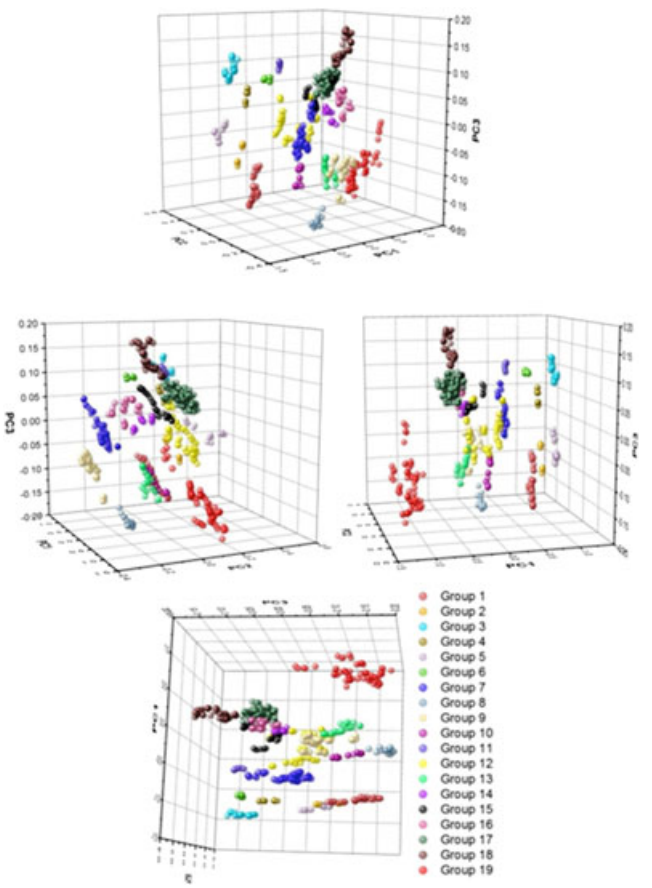

Figure 1. A number of different perspectives of a three-dimensional PCA score plot depicting the distribution of samples based upon their resultant Raman spectra.

vehicle descriptors, including vehicle origin, manufacturer, specific models, year of manufacture and in some instances the manufacturing plant where the vehicle was assembled. A comprehensive summary of the samples that comprise each grouping in the Raman dataset is provided in Table 2.

Based upon the number of groupings, it can be concluded that the stand-alone Raman model is more discriminating than the corresponding earlier IR model, which only discriminated nine groups (Table 3) using predominantly the same sample set of vehicles. The narrow spectral line width in the Raman spectra not only enables the assignment of the band frequency to be more accurate and precise but also ensures minimal band overlap comparative to IR spectra (Fig. 2). These advantageous features of Raman spectra could account for the increased discrimination observed between samples. Moreover, because vibrations of polymer backbones typically do not generate significant changes in the dipole moment but rather create drastic changes in polarisability, Raman spectroscopy is usually more amenable to the analysis of polymeric coatings such as automotive clear coats. As depicted in Fig. 2, all automotive clear coats tend to be comprised of the same chemical components (i.e. acrylic, melamine, styrene and polyurethane), with variations in the spectra arising from differences in the relative abundance of these constituents in the system.

Table 2. Summary of the samples contained within each grouping following PCA of the Raman spectral dataset

Class no.	No. of samples	Vehicles represented
Class 1	8	US (Dodge/Jeep)
Class 2	2	Mexico (Dodge)
Class 3	6	Japan (Subaru/Nissan)
Class 4	2	Germany (Ford Mondeo)
Class 5	3	South Korea (Holden), Japan (Mitsubishi Colt)
Class 6	3	BMW
Class 7	12	Japan (Mazda/Mitsubishi Lancer/Toyota)
Class 8	4	Australia (Toyota)
Class 9	9	Japan (Mazda/Toyota)
Class 10	4	Mitsubishi Pajero
Class 11	2	SsangYong
Class 12	13	Thailand (Nissan/Toyota), Honda, Suzuki
Class 13	5	Hyundai
Class 14	3	Sweden (Saab), UK (Jaguar)
Class 15	5	Australia (Holden/HSV) [2001–2004]
Class 16	6	Germany (Ford Focus)
Class 17	29	Australia (Holden/HSV) [2009–present]
Class 18	10	Australia (Holden/HSV) [2004–2009]
Class 19	13	Australia (Ford), Spain (Nissan)

Table 3. Summary of vehicles grouping from the 2012 IR dataset[32]

Class 0	Australia – Ford
Class 1	Japan – Mazda, Mitsubishi Lancer, Toyota
Class 2	South Korea
Class 3	Australia – Holden
Class 4	Japan – Honda, Mitsubishi Pajero, Subaru, Suzuki
Class 5	Mexico
Class 6	Thailand
Class 7	Germany – Ford Focus
Class 8	USA

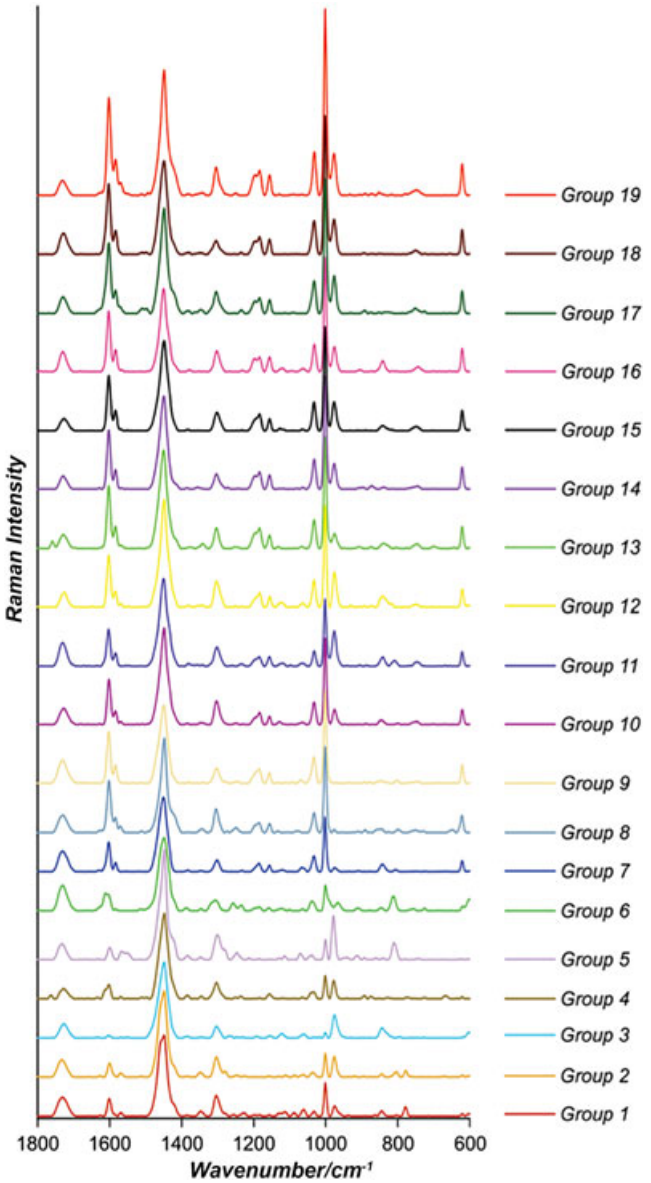

Figure 2. Raman spectra obtained from the centroid of each PCA grouping.

The factor loadings for the first three PCs were examined to identify spectral regions responsible for the discrimination of samples on the score plot. The loading plot for PC1, shown in the Fig. 3, revealed two peaks of significant positive correlation ca. 1602 and 1002 cm^{-1}. The peak at approximately 1602 cm^{-1} is part of a doublet of bands indicative of ring stretching attributable to styrene. Similarly, the intense, sharp peak at roughly 1002 cm^{-1} is characteristic for trigonal ring breathing also ascribable to styrene. Consequently, the discrimination between samples on PC1 is primarily attributable to the abundance of styrene in the clear coat. For example, samples in classes 1–6, as can be seen from Fig. 3, have a relatively low abundance of styrene in the clear coat and thus attain significant negative scores on PC1. Conversely, samples obtained from the Australian-manufactured Ford and Spanish-made Nissan vehicles of class 19 have comparatively larger intensities of these peaks than the other samples and subsequently have larger positive scores on PC1.

Journal of RAMAN SPECTROSCOPY

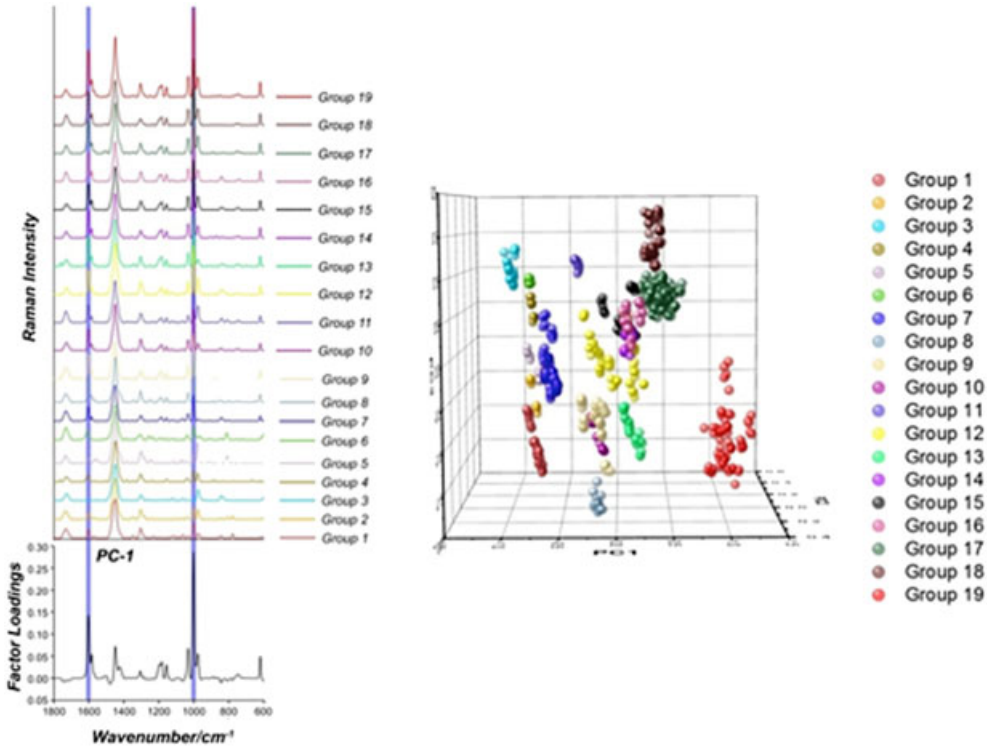

Figure 3. Factor loading plot for PC1. The blue regions superimposed on the representative Raman spectra for each grouping denote spectral regions significantly positively correlated with PC1.

The loading plot for PC2, depicted in Fig. 4, revealed regions of positive correlation ca. 1447, 1425 and 977 cm^{-1}. Additionally, there was also a peak of significant negative correlation at approximately 1004 cm^{-1}, which denotes a slight band shift in the peak indicative of trigonal ring breathing characteristic of styrene. This signifies that PC2 is accounting for a subtle variation in the wavenumber shift of the styrene peak, suggesting a slight modification to the styrene binder, presumably because of the chemical

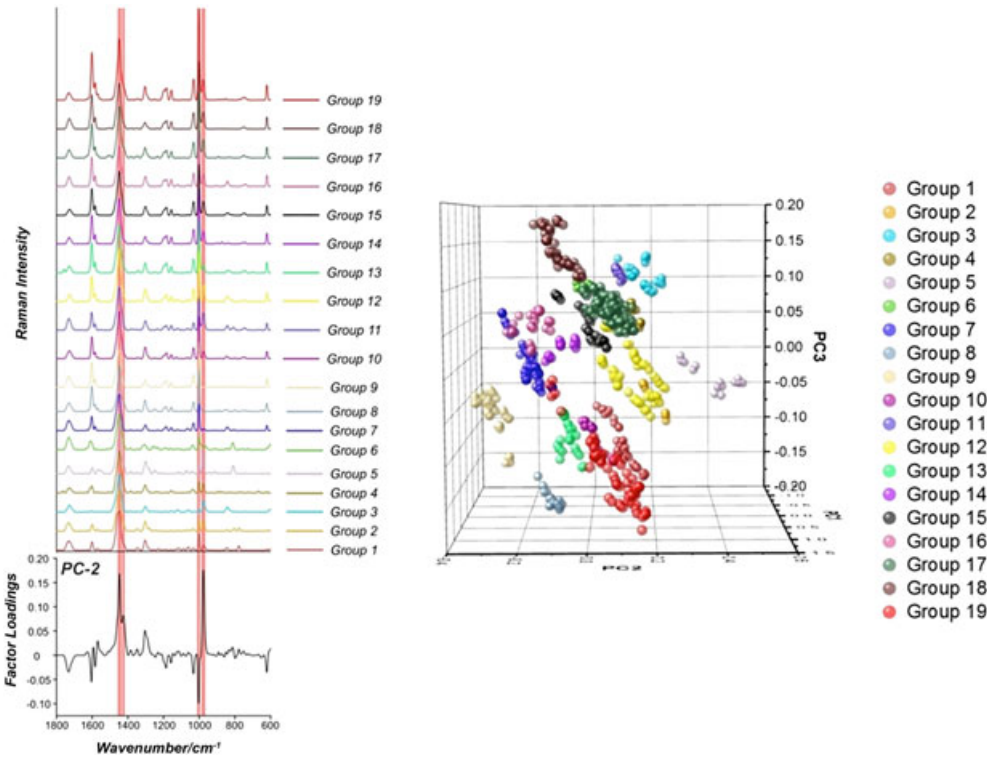

Figure 4. Factor loadings plot for PC2. The red zones overlaid on the Raman spectra obtained from each class centroid, signify regions of substantial correlation with PC2.

component it is linking or polymerising with. The large positive loading at approximately 1447 cm^{-1} signifies CH_3 and CH_2 deformations that may be attributed to the acrylic backbone. Similarly, the positive loading at 1425 cm^{-1}, which corresponds to a shoulder on the main acrylic peak at 1447 cm^{-1}, is indicative of the methylene (=CH_2) deformation vibration also characteristic for certain acrylic polymers. Finally, the significant positive loading at approximately 977 cm^{-1} signifies the triazine ring breathing of the melamine cross-linking agent. Consequently, samples are differentiated on PC2 based upon the presence and intensity of acrylic peaks at 1447 and 1425 cm^{-1} and the melamine peak at 977 cm^{-1}, in addition to a slight band shift variation of the main diagnostic peak for styrene. For example, samples that attain large positive scores on PC2 (e.g. class 5) have relatively large intensities of peaks at 1447, 1425 and 977 cm^{-1}, including no band shift in the styrene peak. Conversely, samples with large negative scores on PC2 (e.g. class 9) have relatively low intensities of the acrylic (1447 and 1425 cm^{-1}) and melamine (977 cm^{-1}) peaks and or a large intensity of the band-shifted styrene peak (1004 cm^{-1}).

The factor loadings for PC3, depicted in Fig. 5, revealed peaks of significant positive correlation at 1613 and 977 cm^{-1}, in addition to regions of large negative correlation at 1449 and 1305 cm^{-1}. The large negative loadings at 1449 and 1305 cm^{-1} can be assigned to the CH_3 and CH_2 deformations and CH_2 in-phase twisting vibrations of the acrylic component respectively. Interestingly, the negative loading *ca.* 1449 cm^{-1} represents a slight band shift in the acrylic peak, most likely inferring variation in the acrylic co-polymer utilised to form the backbone. As described previously, the large positive loading at approximately 977 cm^{-1} is indicative of triazine ring breathing of melamine. Finally, the large positive loading at approximately 1613 cm^{-1} corresponds to a shoulder on the larger doublet peak ca. 1602 cm^{-1} that was previously assigned to the quadrant ring stretching of styrene. This shoulder can also be attributed to ring stretching of aromatics, most likely from modifications to the styrene binder or from other aromatic additives (e.g. xylene and methylbenzenes). Therefore, separation of samples on PC3 is achieved based upon the relative intensities of peaks characteristic for the cross-linking agent melamine, acrylic and styrene binder. For example, samples from classes 8 or 19 attain large negative scores on PC3, based upon the relatively more intense peaks ca. 1449 and 1305 cm^{-1}, signifying either a larger abundance or a specific combination of acrylic binder/s. Importantly, the distinction between the samples in the two Australian-made Holden groupings (classes 17 and 18) can be made based upon the position of these samples on PC3. The samples from class 17, which represents Holden vehicles manufactured from 2009 onwards, attain less positive scores on PC3 than the samples from class 18 (Holden vehicles manufactured between 2004 and 2009). These samples from class 17 have comparatively less positive scores on PC3 because of the more intense vibrational bands at approximately 1449 and 1305 cm^{-1}. This suggests that the samples from class 17 most likely have a much larger abundance of the same acrylic binder or have a different acrylic backbone than those in class 18.

A LDA model was generated by utilising the first three PCs and the groupings derived from PCA of the calibration data. The three PC score LDA model successfully classified 96.9% of the data in the calibration set, with only threee samples and their corresponding replicates being misclassified (Table S1 (Supporting Information)). Two of the three samples misclassified were obtained from a Japanese-manufactured Suzuki Grand Vitara and a Honda Civic made in the UK. Both samples were visually projected into class 12; however, the model predicted these samples to be classified in classes 15 and 14 respectively. Whilst these samples were misclassified, it is important to note that these samples represent singular vehicles in the dataset and are thus not well defined in the model and cannot be verified. Hence, at this time, the model

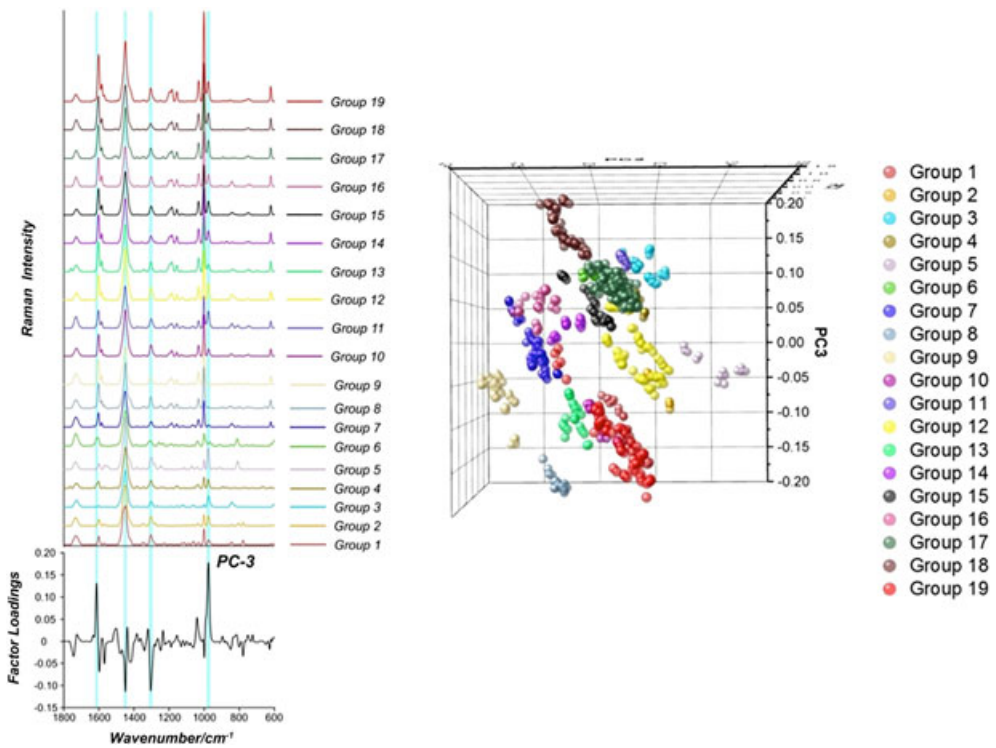

Figure 5. Factor loading plot for PC3. The light blue regions superimposed on the representative Raman spectra of each PCA grouping denote spectral regions significantly correlated with PC3.

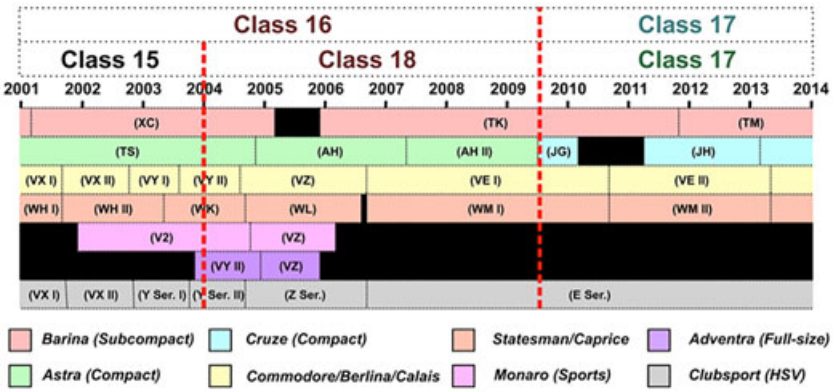

Figure 6. Timeline of select lines of Holden vehicles. The red dashed line denotes the demarcation between samples in groupings 15, 17 and 18 of the Raman statistical model.

cannot be used to reliably assign vehicles to some classes. However, it does demonstrate the potential of FT-Raman spectroscopy in this context and if, over time, as the size of the model increased and, more importantly, the number of samples representing these vehicles increased, then specific groupings representing these vehicles may be formed. This proof of concept however does demonstrate the potential of a Raman spectral database for forensic automotive paint analysis.

Although these samples are not adequately defined in the model, they still need to be classified into one of the pre-specified groupings, thus accounting for their misclassification. The final misclassified sample in the calibration set was obtained from a Holden VE Commodore manufactured in 2007. Whilst the sample should group with the other samples in class 18, the LDA model classifies the sample into group 17 with the Holden vehicles made from 2009 onwards. Inspection of Fig. 3 highlights that spectra from groups 17 and 18 only differ in the relative intensities of weak bands near 1530, 1370 and 1170 cm^{-1}, which explains the close proximity of the groups in the three-dimensional LDA space. Their centroid discriminant values are separated by only 15.8, whilst the next nearest group is 100 away from them. The discriminant values, 5.3–6.6 (class 17) and 8.3–11.2 (class 18), clearly place this sample near the midway point between the groups. Thus, the misclassification is most likely because of the variance in the sample spectra. Whilst the assignment to class 17 has the higher probability, potential assignment to class 18 cannot be rejected with 95% or greater confidence. This underscores the requirement that all assignment LDA scores should be critically examined before accepting or rejecting assignments. It should also be remembered that LDA will assign a class to any sample submitted to it, even if it is a gross outlier or its type has not been included in the calibration set. Examination of the discriminant values will again bring such samples to a user's attention.

The LDA model successfully classified 97.6% of the data in the test set, with only one sample and the corresponding replicates being misclassified (Table S2 (Supporting Information)). The sample in question was obtained from a Thai-manufactured Toyota Hilux vehicle from class 12, which was classified by the model into class 15. Again, this was from classes with few vehicles (3 and 4 respectively) and are hence not as well defined as classes with greater numbers of samples (e.g. Holden (Commodore, etc.) – 39 and Australian Ford – 17). Whilst some samples were misclassified, it can be concluded that the overall performance of the model is highly discriminating, with only minimal overlap between select groupings. From a comparative standpoint, the classification accuracy of the IR model is slightly greater than the equivalent model generated from Raman data. This can most likely be attributed to the fact that there are more overall groupings in the Raman model, indicating that there is a potential for more overlap between the groupings. Additionally, it is worth noting that because of differences in the number and structure of the groupings, an effective comparison of the predictive performance between the two models could not be made, as the samples used to constitute the calibration and validation sets were different.

Conclusions

The model generated from Raman data is potentially more discriminating than the equivalent clear coat model obtained from IR data for the same sample set of vehicles.[32] This is best exemplified by the discrimination between the Australian-made Holden and HSV vehicles. In the IR model, there are only two groupings in the dataset representing these vehicles: samples signifying vehicles manufactured prior to mid-2009 and samples denoting vehicles manufactured after this time period. However, in the Raman model, the samples contained in the prior mid-2009 class of the IR model are further subdivided into two distinct groupings. The samples in class 15 of the Raman model signify vehicles manufactured from a time period between 2001 until the end of 2003. The samples in class 18 represent Holden vehicles manufactured from the start of 2004 until mid-2009. This potentially enables increased discrimination between Holden and HSV vehicle models, which would not otherwise be discerned from the IR model. Figure 6 depicts a timeline highlighting the production years of specific vehicle models under the General Motor's Holden umbrella. The dashed red lines on the timeline denote the points of distinction between the sample groupings in the Raman dataset. This work highlights the complementary nature of IR and Raman spectroscopy for forensic analysis of automotive clear coats. That being so, it should still be born in mind that this is only clear coat information, and other information that may be available, such as basecoat colour, should be considered in conjunction with any vibrational spectral data.

Acknowledgements

Mark Maric was supported by an Australian Postgraduate Award. The authors thank Georgina Sauzier (Curtin University) for reviewing drafts of the paper.

References

[1] Scientific Working Group for Materials Analysis (SWGMAT), Forensic science communications **1999**, 1.
[2] ASTM E-1610-02, ASTM International: Pennsylvania, **2002**.
[3] K. P. Kirkbride, V. Otieno-Alego, in *Expert Evidence* (Eds: H. Selby, I. Freckelton), Thomson Reuters, London, **2010**.
[4] C. Muehlethaler, L. Gueissaz, G. Massonnet, in *Encyclopedia of Forensic Sciences* (Eds: J. A. Siegel, P. J. Saukko), Academic Press, London, **2013** p, 265.
[5] Science and Technology Committee, The Forensic Science Service, **2011**.
[6] National Academy of Sciences, Strengthening forensic science in the United States: a path forward, National Research Council, **2009**.
[7] S. L. Morgan, E. G. Bartick, *Forensic Analysis on the Cutting Edge*, John Wiley & Sons, West Sussex, **2007** p, 333.
[8] G. Zadora, in *Encyclopedia of Analytical Chemistry* (Ed: R. A. Meyers), John Wiley & Sons, West Sussex, **2006**.
[9] G. Zadora, A. Martyna, D. Ramos, C. Aitken, *Statistical Analysis in Forensic Science: Evidential Value of Multivariate Physicochemical Data*, John Wiley & Sons, West Sussex, **2014**.
[10] E. M. Enlow, J. L. Kennedy, A. A. Nieuwland, J. E. Hendrix, S. L. Morgan, *Appl. Spectrosc.* **2005**, *59*, 986.
[11] S. L. Morgan, A. A. Nieuwland, C. R. Mubarak, J. E. Hendrix, E. M. Enlow, B. J. Vasser, E. G. Bartick, in Proceedings of the European Fibres Group, Prague, **2004**.
[12] E. J. Reichard, J. V. Goodpaster, *Chemometrics applied to the discrimination of synthetic fibres by microspectrophotometry*, Purdue University, West Lafayette, IN, **2013**.
[13] M. N. C. Grainger, M. Manley-Harris, S. Coulson, *J. Anal. Atomic Spectrom.* **2012**, *27*, 1413.
[14] C. D. May, R. J. Watling, *Forensic Sci. Med. Pathol.* **2009**, *5*, 66.
[15] A. Kher, M. Mulholland, E. Green, B. Reedy, *Vibrational Spectros.* **2006**, *40*, 270.
[16] N. C. Thanasoulias, N. A. Parisis, N. P. Evmiridis, *Forensic Sci. Int.* **2003**, *138*, 75.
[17] C. S. Lee, T. M. Sung, H. S. Kim, C. H. Jeon, *J. Anal. Appl. Pyrolysis* **2012**, *96*, 33.
[18] N. C. Thanasoulias, E. T. Piliouris, M. E. Kotti, N. P. Evmiridis, *Forensic Sci. Int.* **2002**, *130*, 73.
[19] J. A. Barrett, J. A. Siegel, J. V. Goodpaster, *J. Forensic Sci.* **2011**, *56*, 95.
[20] M. Monfreda, A. Gregori, *J. Forensic Sci.* **2011**, *56*, 372.
[21] P. M. L. Sandercock, E. D. Pasquier, *Forensic Sci. Int.* **2003**, *134*, 1.
[22] P. M. L. Sandercock, E. Du Pasquier, *Forensic Sci. Int.* **2004**, *140*, 43.
[23] W. J. Egan, R. C. Galipo, B. K. Kochanowski, S. L. Morgan, E. G. Bartick, M. L. Miller, D. C. Ward, R. F. Mothershead II, *Anal. Bioanal. Chem.* **2003**, *376*, 1286.
[24] W. J. Egan, S. L. Morgan, E. G. Bartick, R. A. Merrill, H. J. Taylor III, *Anal. Bioanal. Chem.* **2003**, *376*, 1279.
[25] J. M. Feldmann, J. V. Goodpaster, *Discrimination of color copier/laser printer toners by Raman spectroscopy and subsequent chemometric analysis*, Purdue University, West Lafayette, IN, **2013**.
[26] E. G. Udrăştioiu, A. A. Bunaciu, H. Y. Aboul-Enein, I. G. Tănase, *Inst. Sci. Technol.* **2009**, *37*, 230.
[27] A. Kher, M. Mulholland, B. Reedy, P. Maynard, *Appl. Spectrosc.* **2001**, *55*, 1192.
[28] J. V. Goodpaster, A. B. Sturdevant, K. L. Andrews, E. M. Briley, L. Brun-Conti, *J. Forensic Sci.* **2009**, *54*, 328.
[29] J. V. Goodpaster, A. B. Sturdevant, K. L. Andrews, L. Brun-Conti, *J. Forensic Sci.* **2007**, *52*, 610.
[30] B. K. Kochanowski, S. L. Morgan, *J. Chromatogr. Sci.* **2000**, *38*, 100.
[31] E. A. Liszewski, S. W. Lewis, J. A. Siegel, J. V. Goodpaster, *Appl. Spectrosc.* **2010**, *64*, 1122.
[32] M. Maric, W. van Bronswijk, S. W. Lewis, K. Pitts, *Anal. Methods* **2012**, *4*, 2687.
[33] C. Muehlethaler, G. Massonnet, M. Deviterne, M. Bradley, A. Herrero, I. D. de Lezana, S. Lauper, D. Dubois, J. Geyer-Lippmann, S. Ketterer, S. Milet, M. Bertrand, W. Langer, B. Plage, G. Gorzawski, V. Lamothe, L. Marsh, R. Turunen, *Forensic Sci. Int.* **2013**, *229*, 80.
[34] C. Muehlethaler, G. Massonnet, P. Esseiva, *Forensic Sci. Int.* **2011**, *209*, 173.
[35] B. K. Lavine, N. Mirjankar, S. Ryland, M. Sandercock, *Talanta* **2011**, *87*, 46.
[36] B. K. Lavine, A. Fasasi, N. Mirjankar, C. White, J. Mehta, *Microchem. J.* **2014**, *113*, 30.
[37] B. K. Lavine, A. Fasasi, M. Sandercock, *Microchem. J.* **2014**, *117*, 133–137.
[38] B. K. Lavine, A. Fasasi, N. Mirjankar, M. Sandercock, S. D. Brown, *J. Chemometr.* **2014**, *28*, 385.
[39] B. K. Lavine, A. Fasasi, N. Mirjankar, M. Sandercock, *Talanta* **2014**, *119*, 331.
[40] B. K. Lavine, A. Fasasi, N. Mirjankar, C. White, M. Sandercock, *Talanta* **2015**, *132*, 182.
[41] A. Fasasi, N. Mirjankar, R.-I. Stoian, C. White, M. Allen, M. P. Sandercock, B. K. Lavine, *Appl. Spectrosc.* **2015**, *69*, 84.
[42] S. G. Ryland, T. A. Jergovich, K. P. Kirkbride, *Forensic Sci. Rev.* **2006**, *18*, 97.
[43] S. E. J. Bell, S. P. Stewart, W. J. Armstrong, *Infrared and Raman Spectroscopy in Forensic Science*, John Wiley & Sons, West Sussex, **2012** p, 121.
[44] K. Castro, B. Abalos, I. Martínez-Arkarazo, N. Etxebarria, J. M. Madariaga, *J. Cultural Heritage* **2008**, *9*, 189.
[45] T. D. Chaplin, R. J. H. Clark, D. R. Beech, *J. Raman Spectros.* **2002**, *33*, 424.
[46] M. Leona, F. Casadio, M. Bacci, M. Picollo, *J. American Inst. Conservation* **2004**, *43*, 39.
[47] S. E. Bell, L. A. Fido, S. J. Speers, W. J. Armstrong, *Appl. Spectrosc.* **2005**, *59*, 100.
[48] S. E. Bell, L. A. Fido, S. J. Speers, W. J. Armstrong, S. Spratt, *Appl. Spectrosc.* **2005**, *59*, 1333.
[49] S. E. Bell, L. A. Fido, S. J. Speers, W. J. Armstrong, S. Spratt, *Appl. Spectrosc.* **2005**, *59*, 1340.
[50] G. Massonnet, W. Stoecklein, *Sci. Justice* **1999**, *39*, 181.
[51] J. Zięba-Palus, J. Wąs-Gubała, *J. Mol. Struct.* **2011**, *993*, 127.
[52] J. De Gelder, P. Vandenabeele, F. Govaert, L. Moens, *J. Raman Spectros.* **2005**, *36*, 1059.

Supporting Information

Additional supporting information may be found in the online version of this article at the publisher's web site.